Surfaces and Films

Session 5A:
Ion solid interaction, film growth in PVD

Jari Koskinen

Aalto University

Sputtering

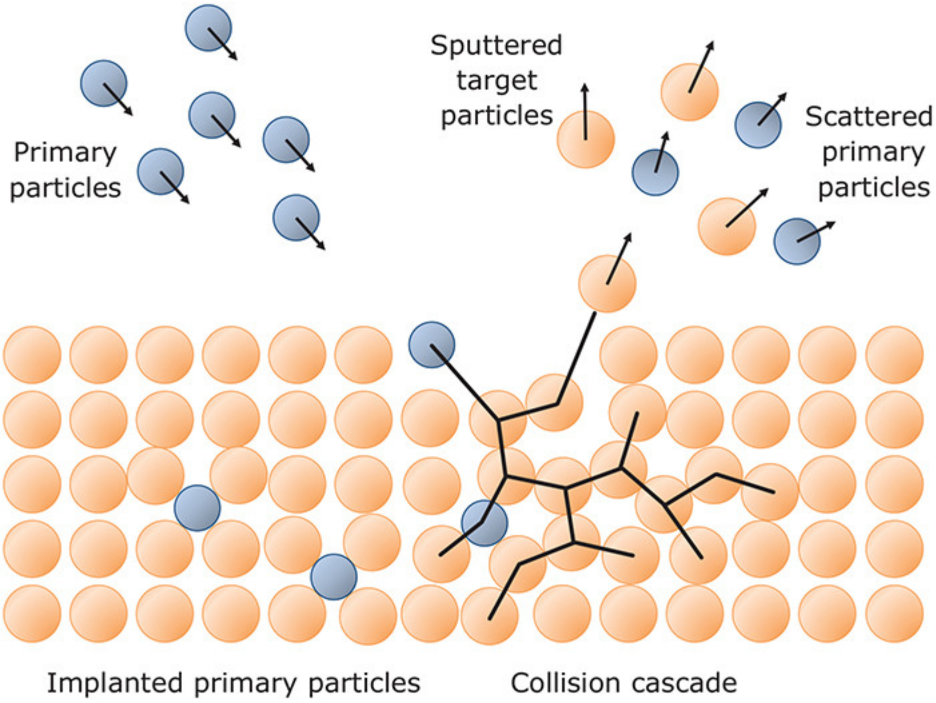
Primary particles
Sputtered target particles
Scattered primary particles
Implanted primary particles
Collision cascade

5 kV Ar-ion hitting Ni (001) surface MD simulation

Kai Nordlund http://www.acclab.helsinki.fi/~knordlun/anims.html

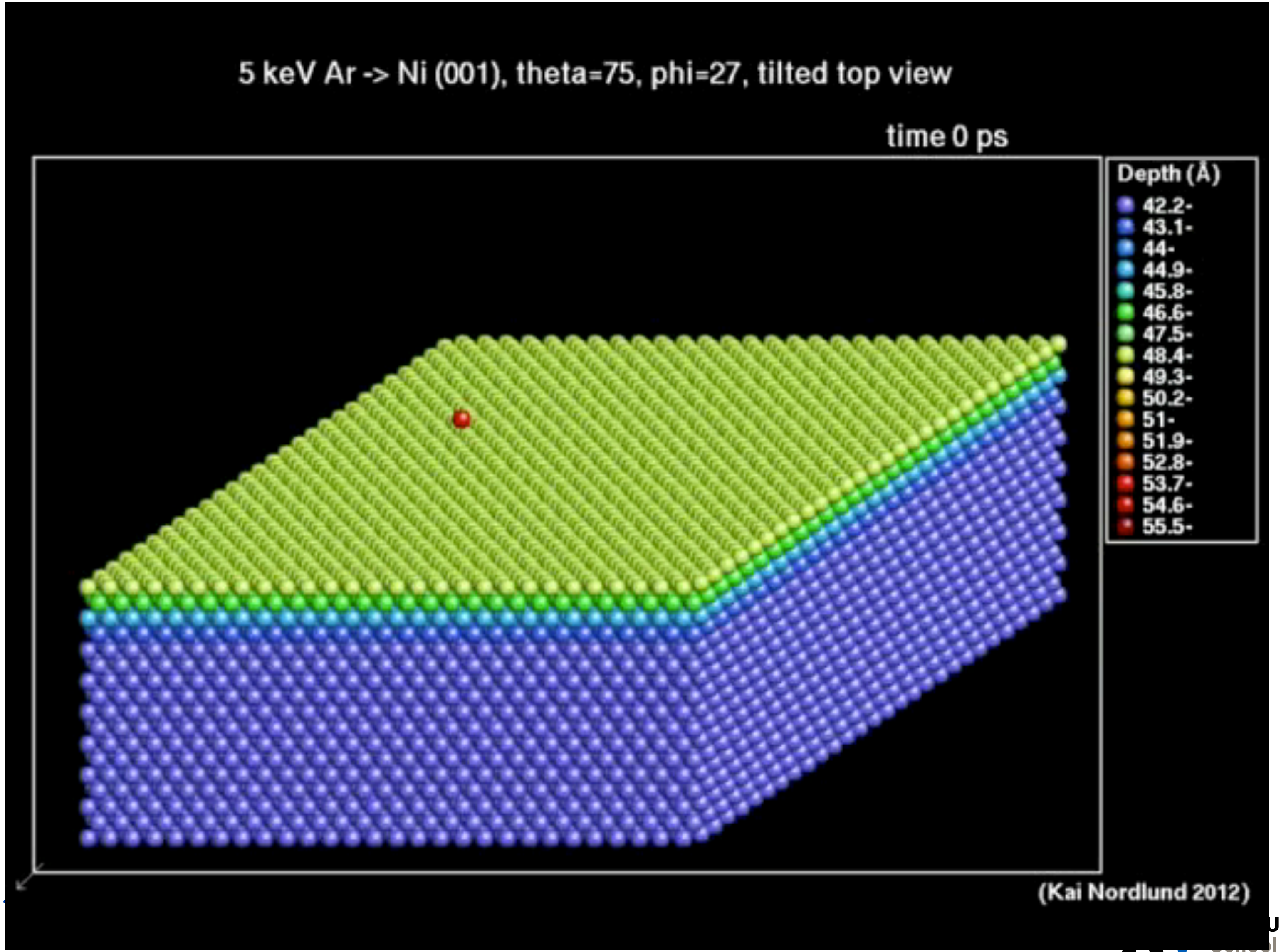

Energetic ion and surface interactions

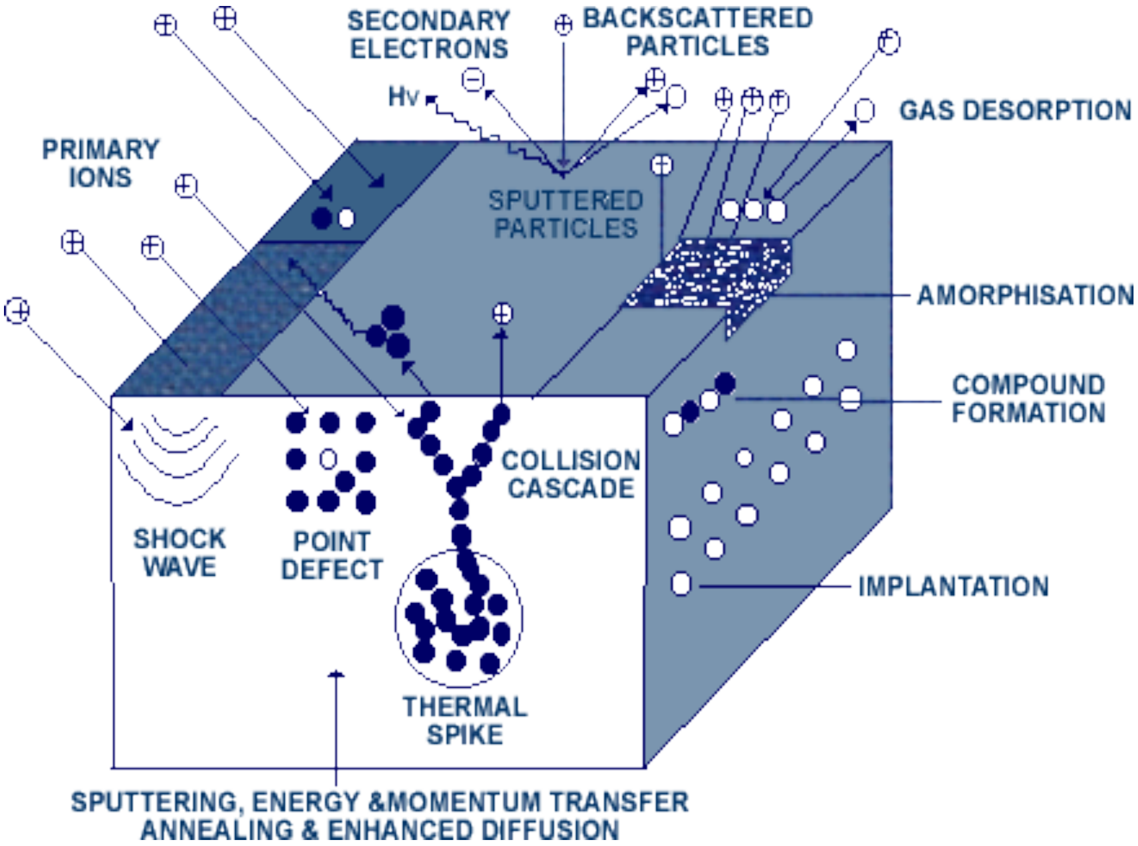

- collision cascade
  $10^{-14} – 10^{-13}$ s
- thermal spike
  $10^{-13} – 10^{-12}$ s
- Fast diffusion
- fast cooling
- relaxation

Kts. simulaatio

Sputtering yield Y

$Y = (\text{outgoing sputtered atoms})_{\text{ave}}/(\text{incoming ions})$

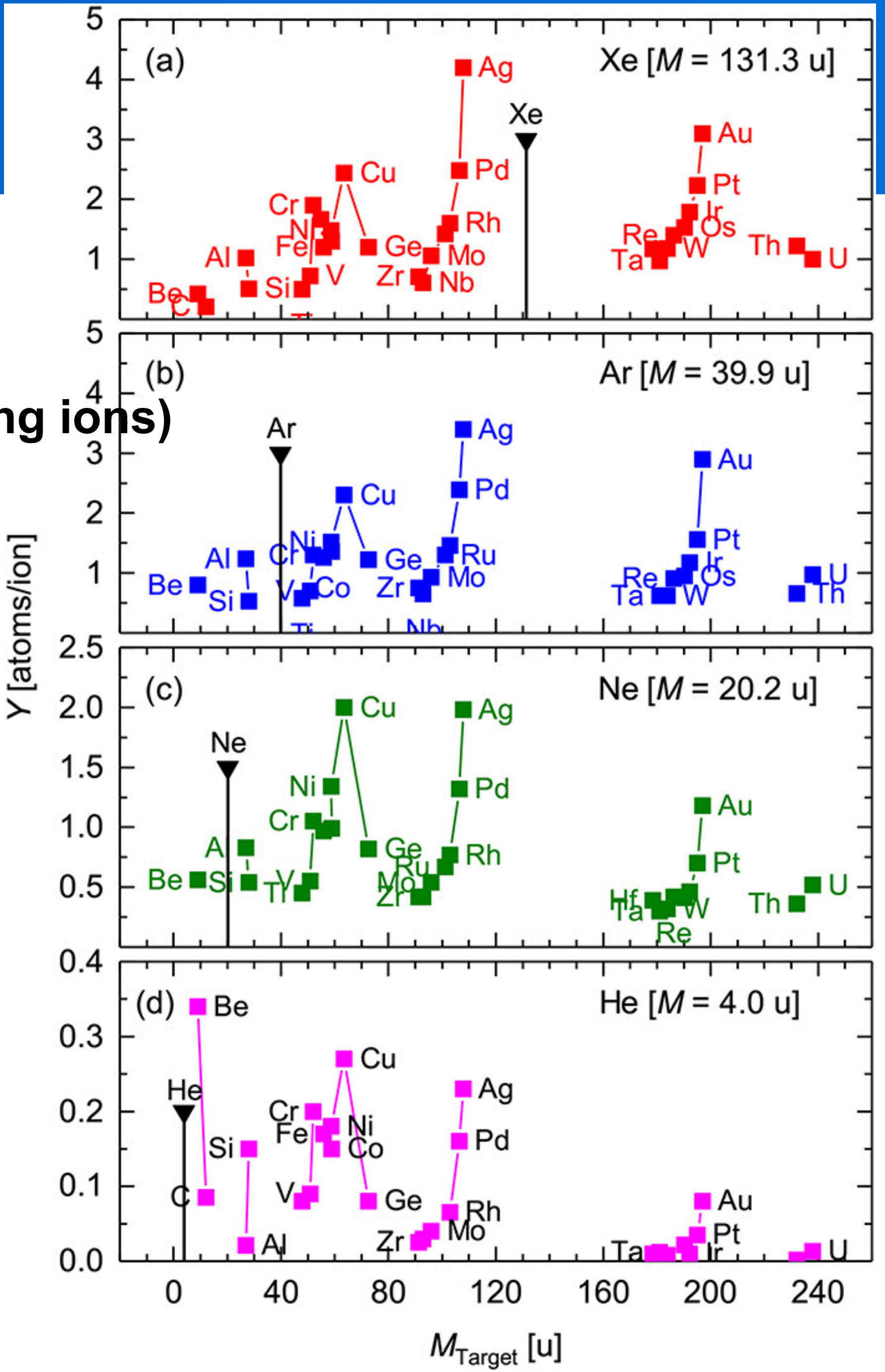

FIG. 7. Sputtering yield Y versus target particle mass M Target for sputtering with Xe ions [panel (a), Ref. 60], Ar ions [panel (b), Ref. 64], Ne ions [panel (c), Ref. 64], or He ions [panel (d), Ref. 60]. E Ion = 600 eV and α = 0 ° . The vertical lines mark the primary ion mass M Ion. Please note the different scales. Modified after Ref. 20.

Published in: Carsten Bundesmann; Horst Neumann; *Journal of Applied Physics* 124, 231102 (2018)
DOI: 10.1063/1.5054046

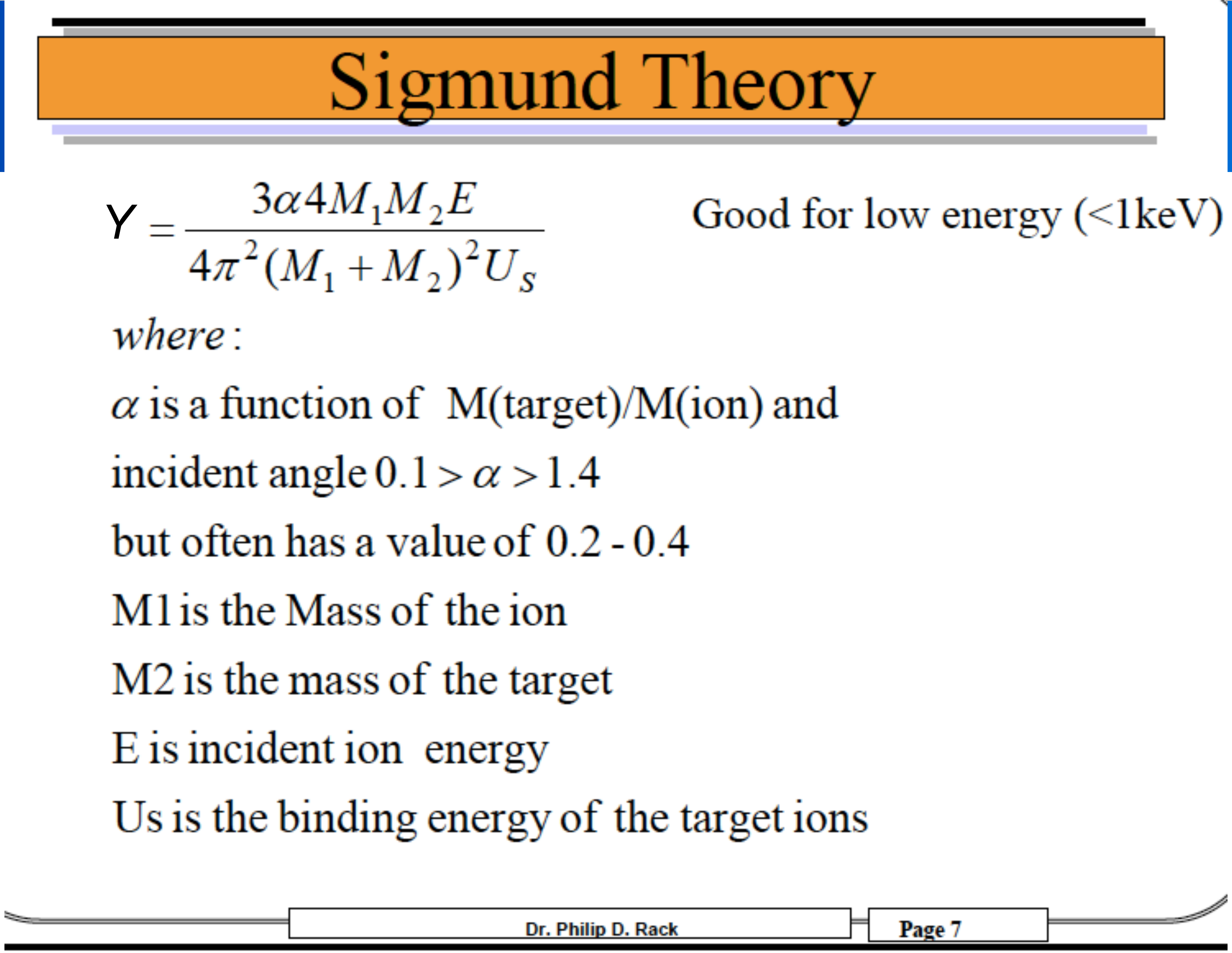

Sigmund Theory

$$Y = \frac{3\alpha 4 M_1 M_2 E}{4\pi^2 (M_1 + M_2)^2 U_S}$$

Good for low energy (<1keV)

$where:$

α is a function of M(target)/M(ion) and

incident angle $0.1 > \alpha > 1.4$

but often has a value of $0.2 - 0.4$

M1 is the Mass of the ion

M2 is the mass of the target

E is incident ion energy

Us is the binding energy of the target ions

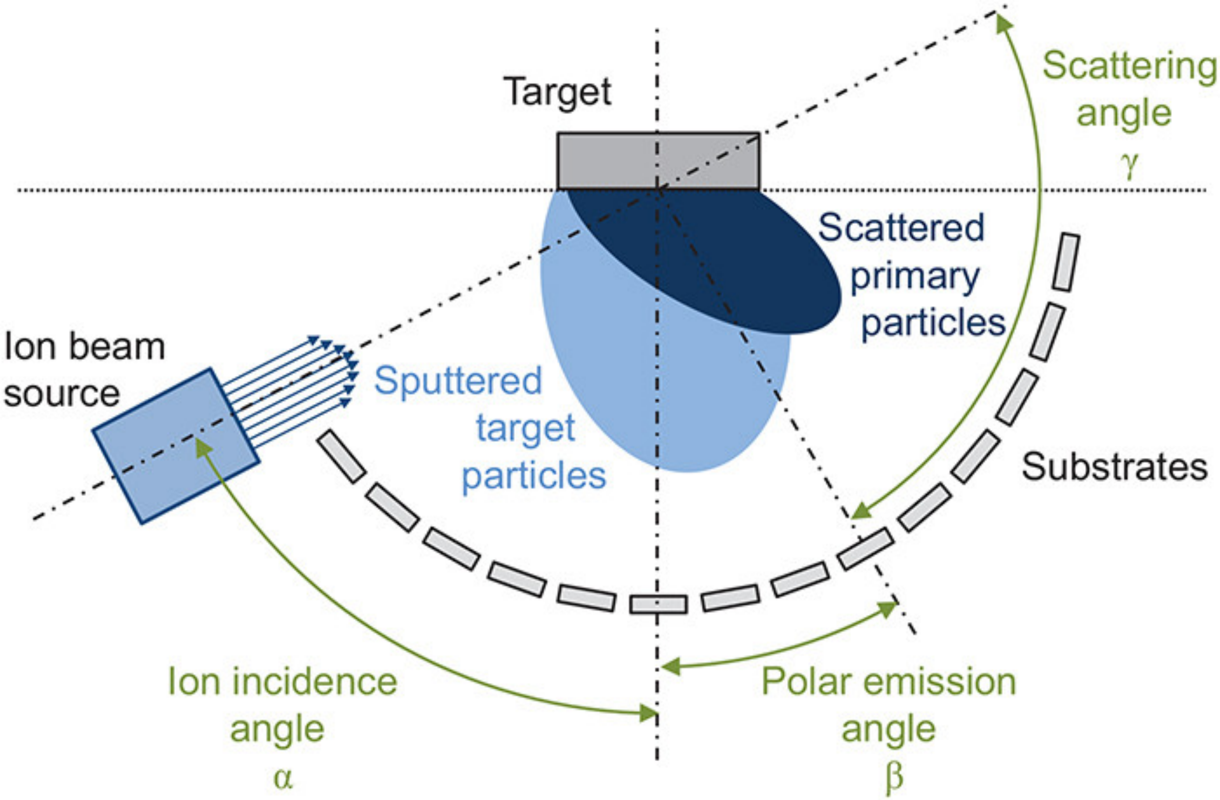

FIG. 14. Schematic drawing of an IBSD setup. Reproduced with permission from Bundesmann et al., Thin Solid Films 589, 487 (2015). Copyright 2015 Elsevier.

Published in: Carsten Bundesmann; Horst Neumann; *Journal of Applied Physics* 124, 231102 (2018)
DOI: 10.1063/1.5054046

Kinetic energy of sputtered ion

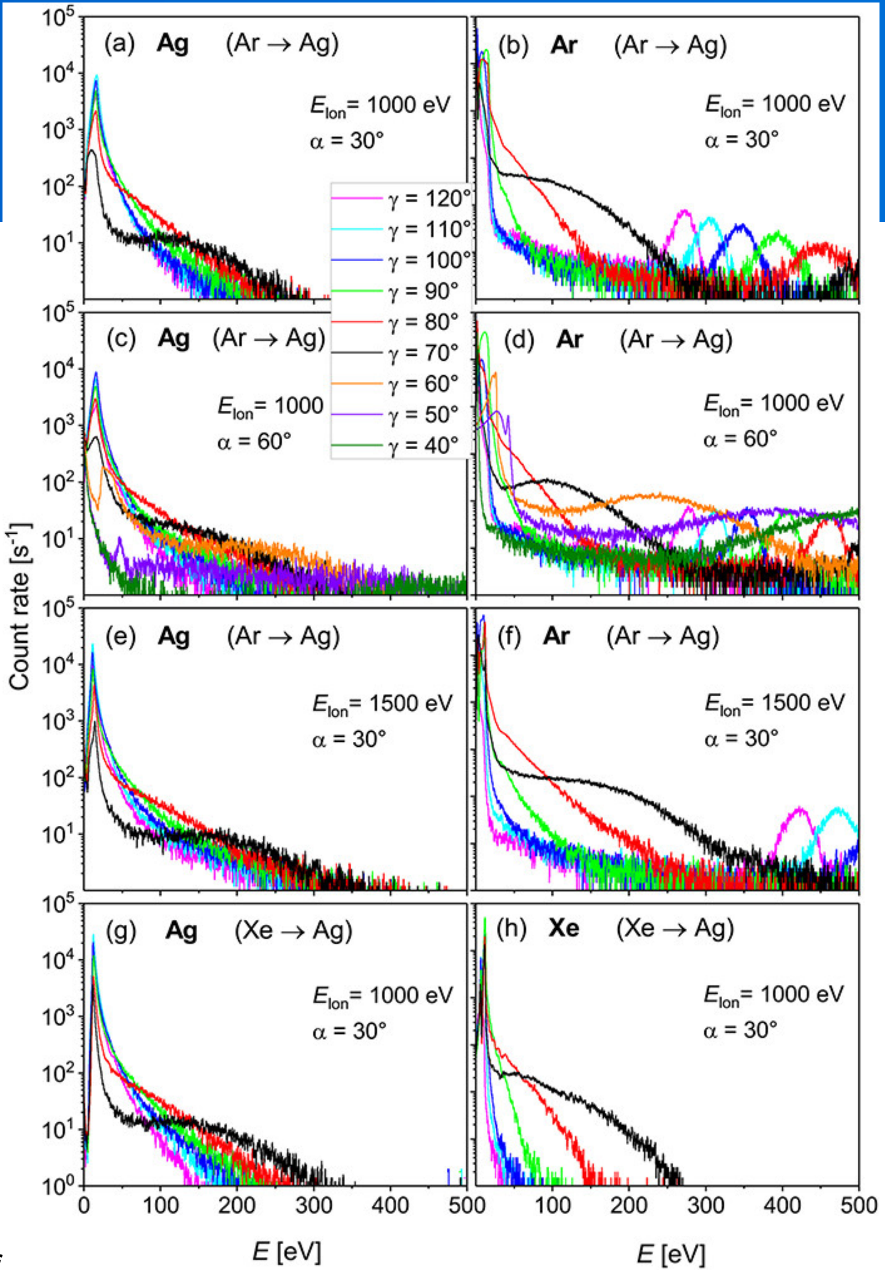

FIG. 18. Measured energy distributions of sputtered target ions [panels (a), (c), (e), and (g)] and scattered primary ions [panels (b), (d), (f), and (h)] in dependence on the scattering angle γ for the bombardment of an Ag target with Ar ions [panels (a)–(f)] or Xe ions [panels (g) and (h)]. The data are shown for different sets of process parameters (E Ion, α). The same line color represents the same scattering angle γ (but not necessarily the same scattering angle β). Reproduced with permission from Bundesmann et al., Contrib. Plasma Phys. 55, 737 (2015). Copyright 2015 Wiley-VCH.

Published in: Carsten Bundesmann; Horst Neumann; *Journal of Applied Physics* 124, 231102 (2018)
DOI: 10.1063/1.5054046

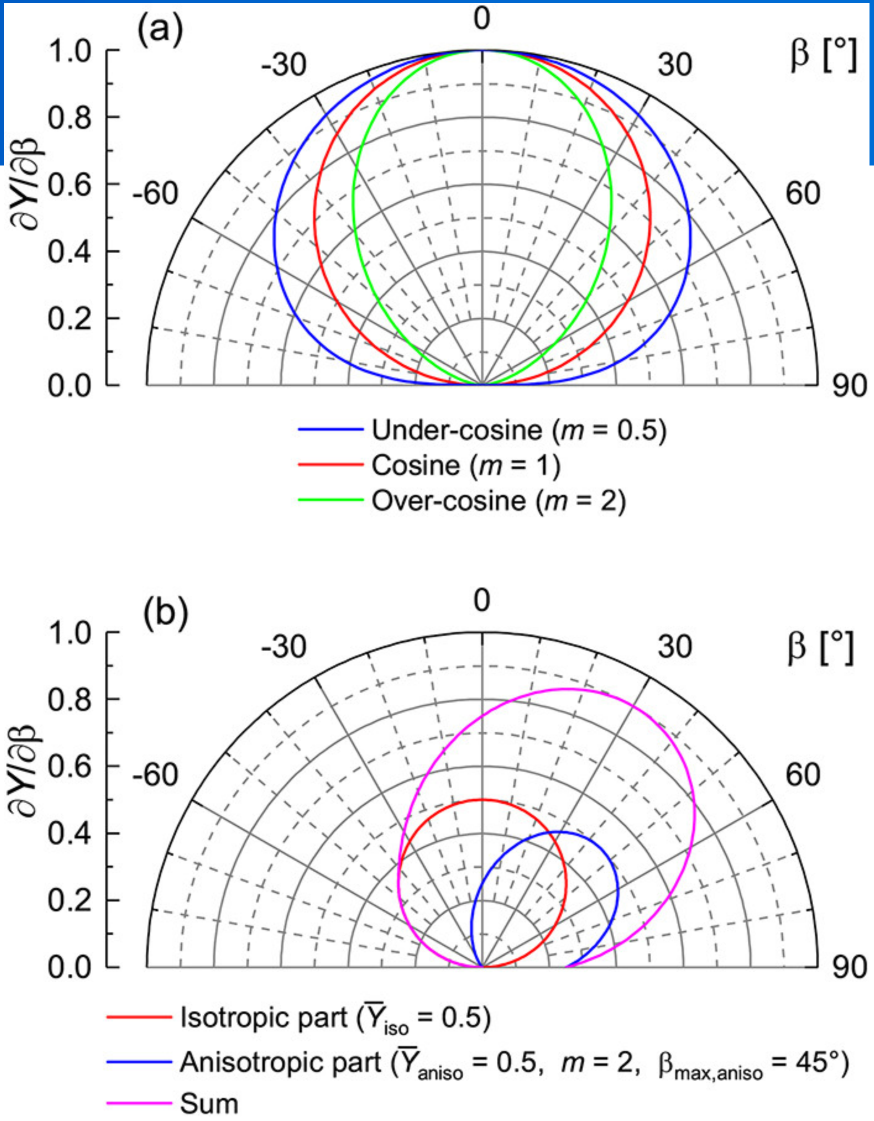

Examples of calculated angular distributions according to Eq. (9) [panel (a)] or Eq. (10) [panel (b)]. The parameters are given below each panel

Sputter yield angle dependence

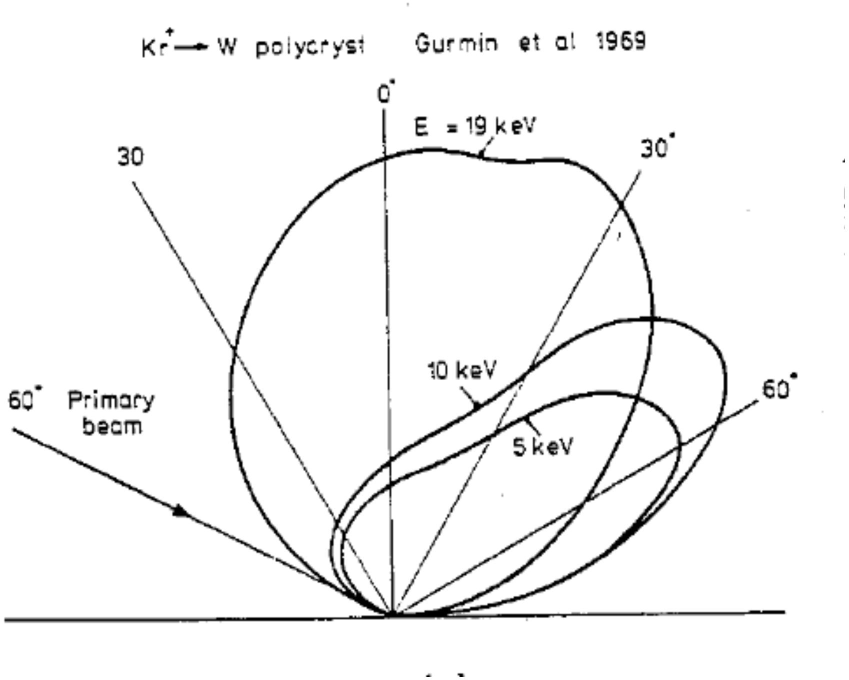

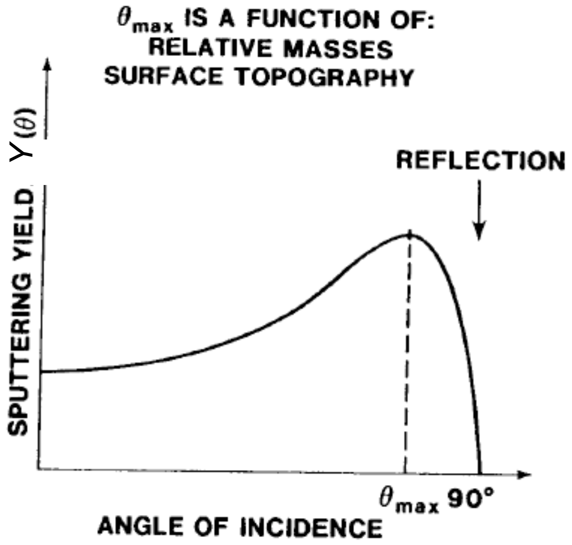

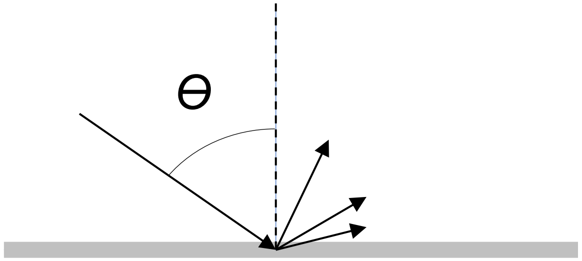

Fraction of Ar sputter ions remain in film (and target)

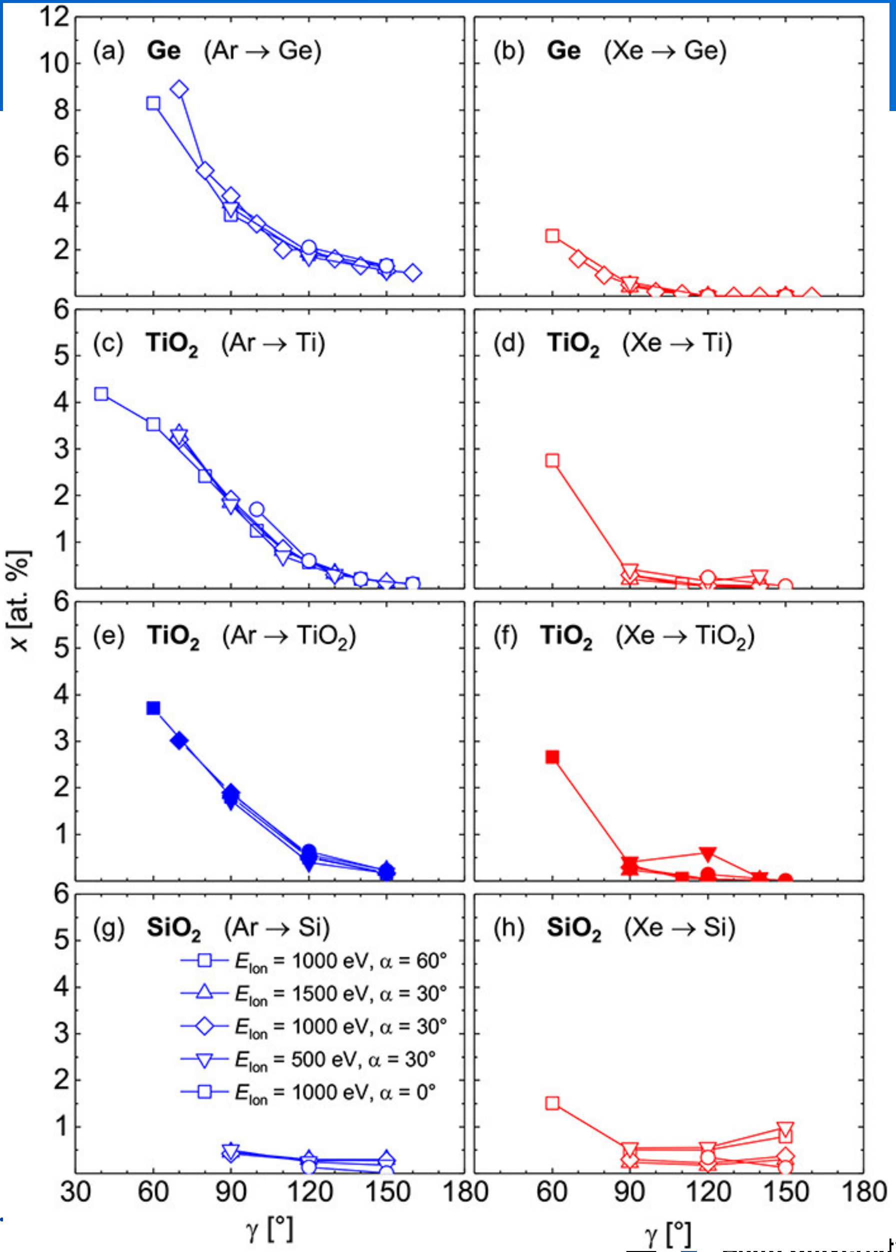

FIG. 21. Atomic fraction x of process gas particles versus scattering angle γ inside Ge thin films [panels (a) and (b)], TiO 2 thin films [panels (c)–(f)], and SiO 2 thin films [panels (g) and (h)] grown by (reactive) IBSD using Ar ions (blue symbols) or Xe ions (red symbols) and a metallic target (open symbols) or a ceramic target (closed symbols). Symbols of the same shape represent the same set of process parameters (E Ion, α). Please note the different scales. Reproduced with permission from Bundesmann et al., Thin Solid Films 589, 487 (2015). Copyright 2015 Elsevier (Ge films); Bundesmann et al., Appl. Surf. Sci. 421, 331 (2017). Copyright 2017 Elsevier (TiO 2 films and Ti target); Bundesmann et al., Eur. Phys. J. B 90, 187 (2017). Copyright 2017 Springer (TiO 2 films and TiO 2 target); Mateev et al., Eur. Phys. J. B 91, 45 (2018). Copyright 2018 Springer (SiO 2 films).

Published in: Carsten Bundesmann; Horst Neumann; *Journal of Applied Physics* 124, 231102 (2018)
DOI: 10.1063/1.5054046
Copyright © 2018 Author(s)

- **Film growth mechanisms**

PVD (Physical Vapour Deposition)

- Material from solid or gas
- Plasma
- Energetic ions hit surface
- Ions and neutrals grow the film

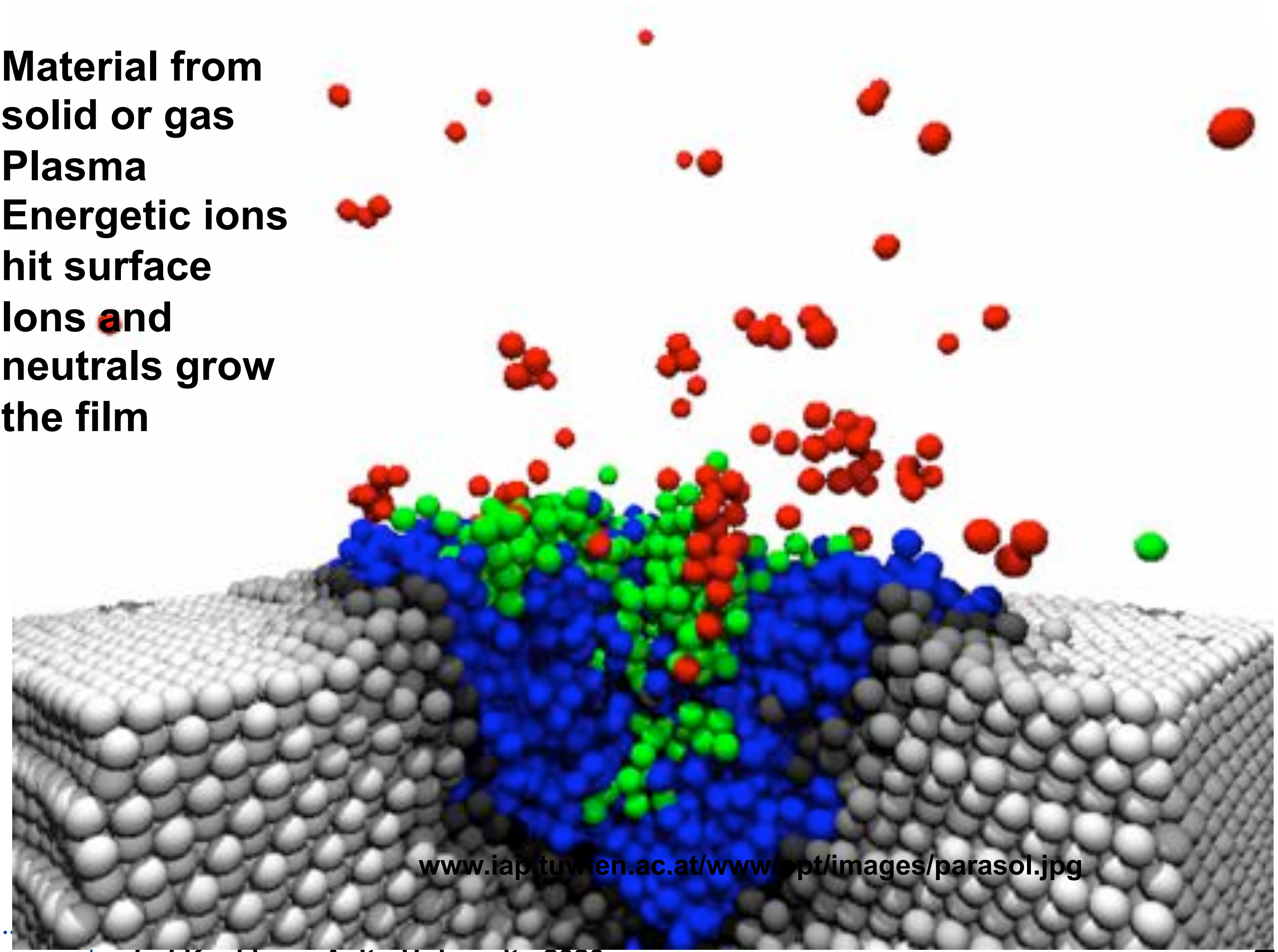

www.iap.tuwien.ac.at/www/opt/images/parasol.jpg

Carbon thin films growth MD simulation
50 eV

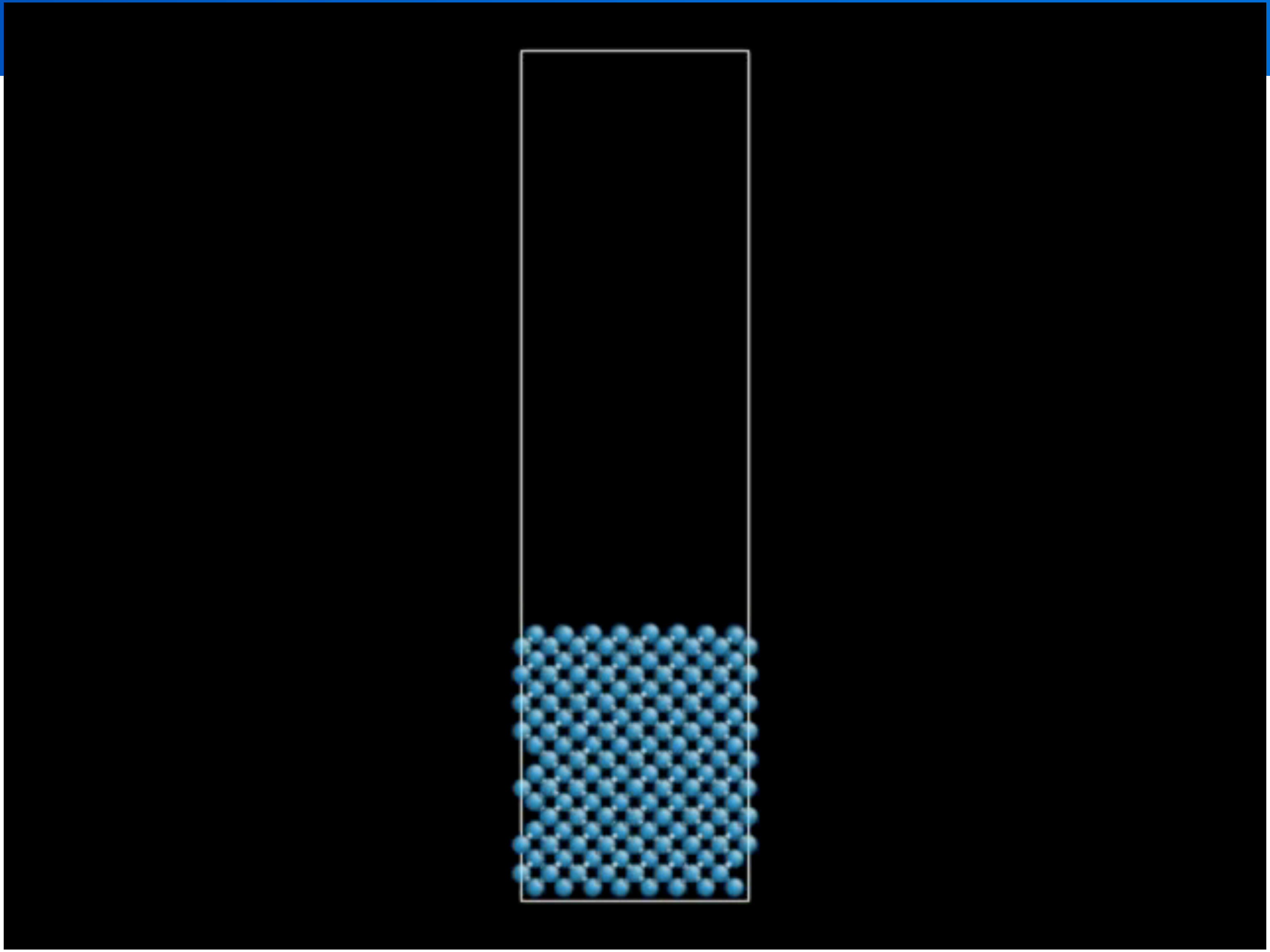

PVD growth process

- Ion energy E_i 10 - 1000 eV
- Surface temperature -190° C - 500° C (normally < 200° C)
- incidence angle
- Ion density
- Gas pressure
- Substrate surface
  - Chemistry
  - Impurities
  - Topography

Coating structure and plasma parameters

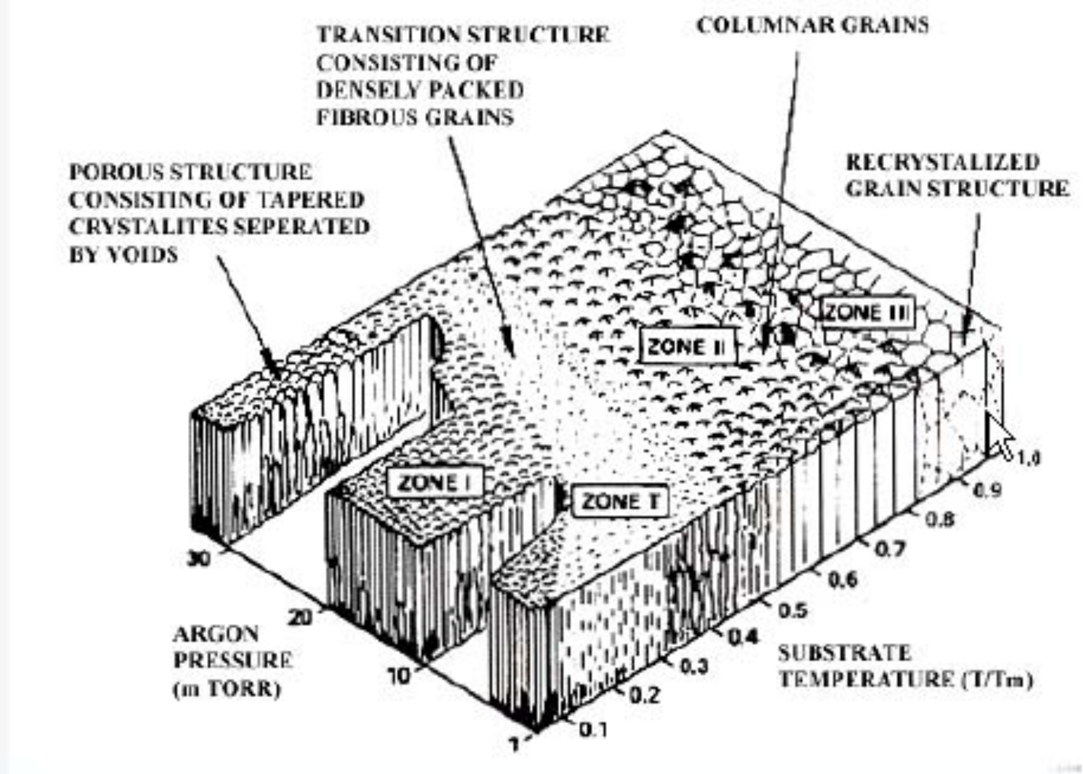

The Thornton Structure Zone Model

Coating structure and plasma parameters

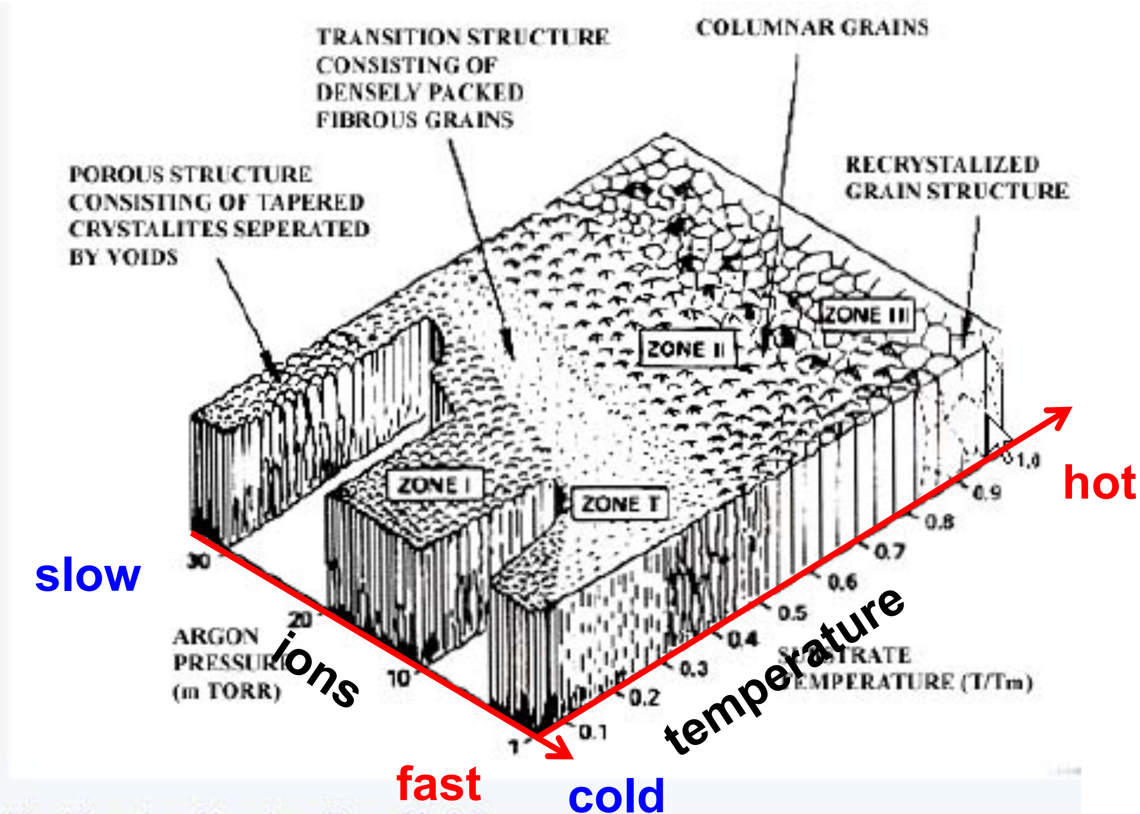

The Thornton Structure Zone Model

Coating structure and plasma parameters

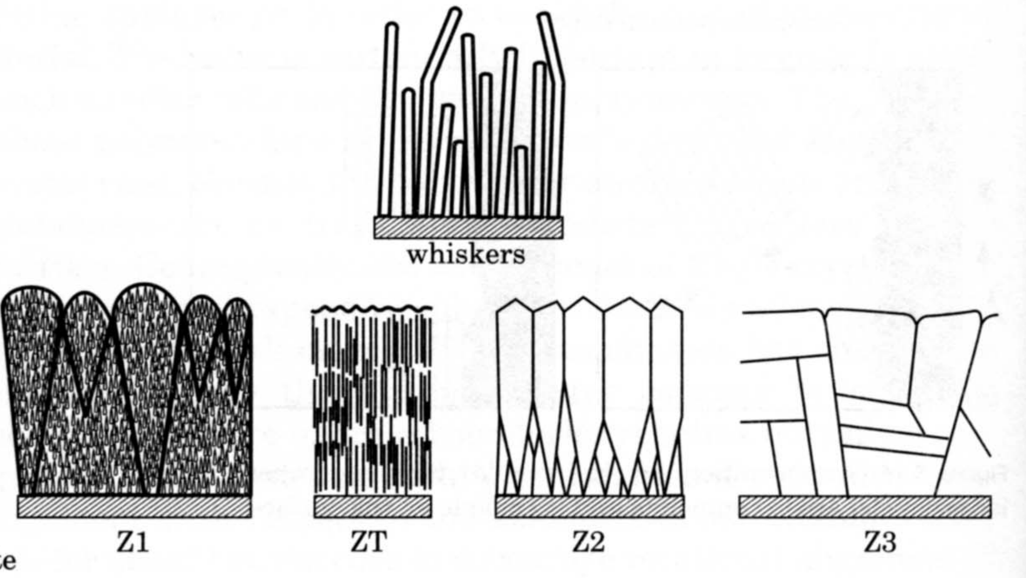

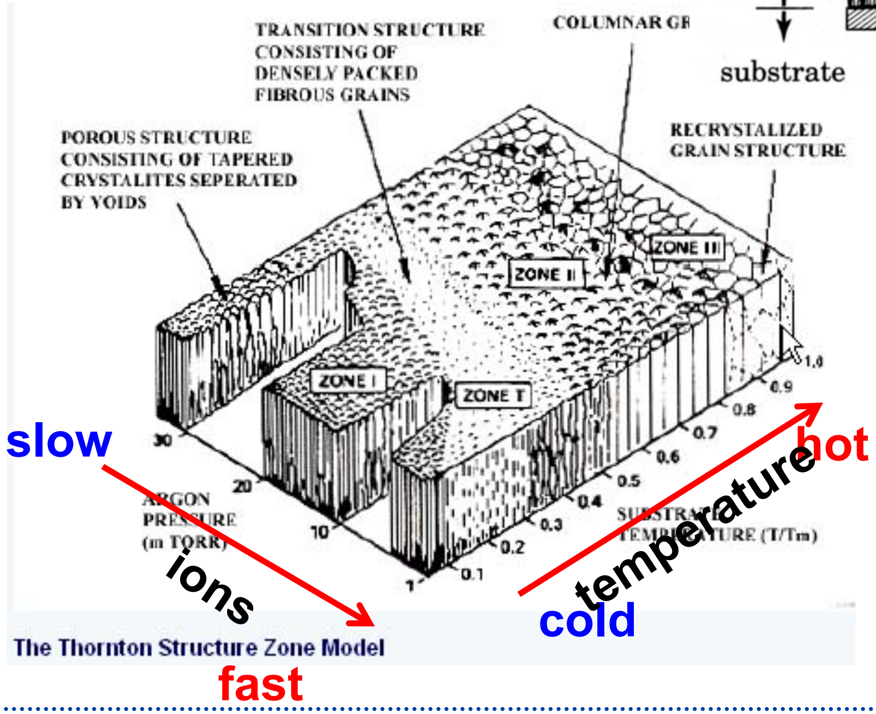

The Thornton Structure Zone Model

Subplantation

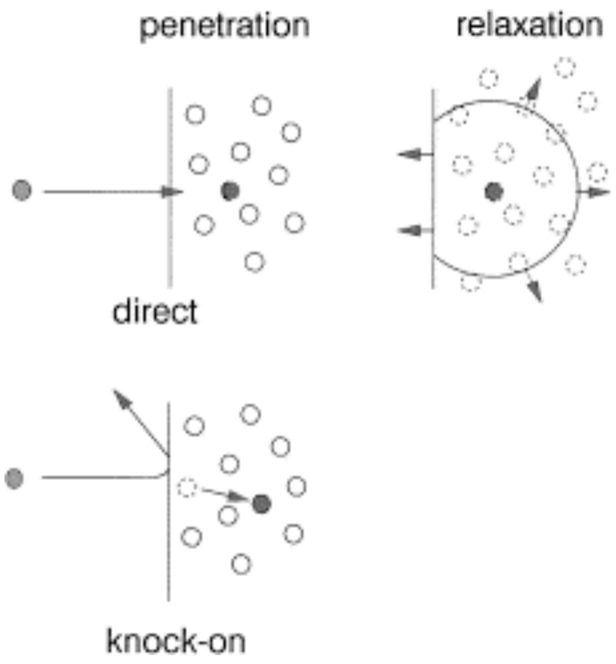

J. Robertson/Materials Science and Engineering R 37 (2002) 129–281

Competition of growing crystals

Handbook of Deposition Technologies for Films and Coatings - Science, Applications and Technology (3rd Edition)
Edited by: Martin, Peter M. © 2010 William Andrew Publishing

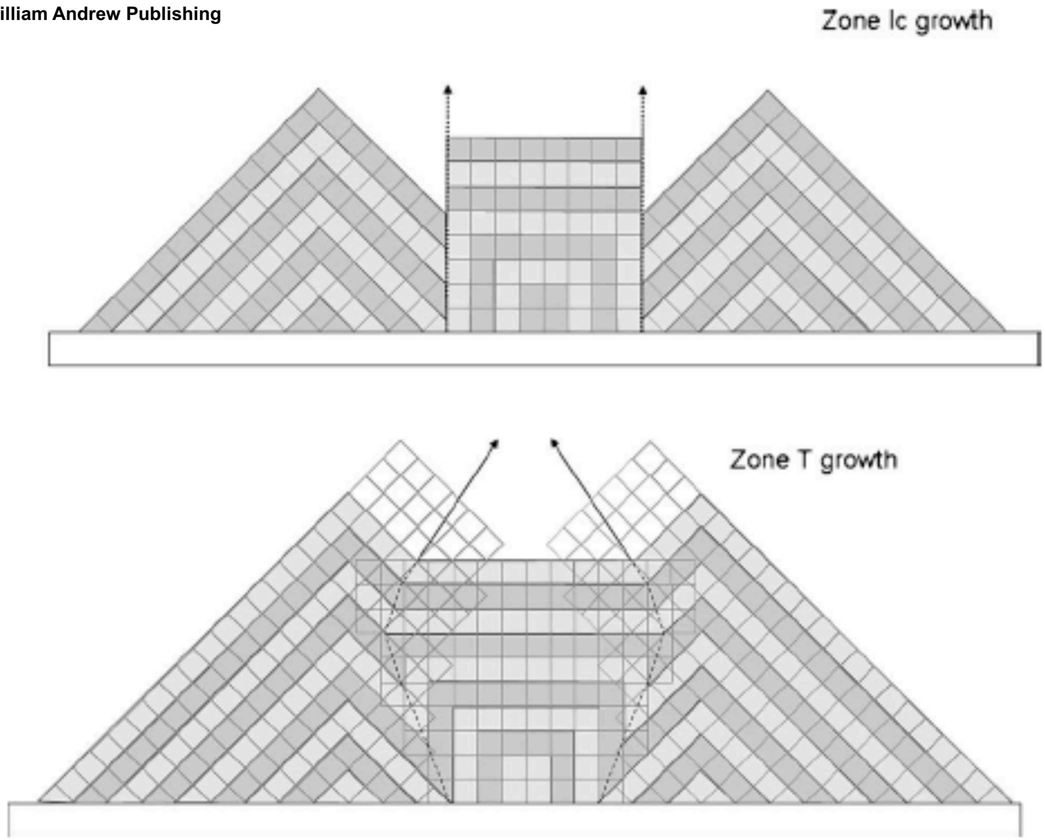

Figure 5.21: Schematic comparison between zone Ic and zone T growth. To indicate the identical normal growth rate of the planes of both grains, alternating coloring is used. In zone T, an overgrowth of one grain by an adjacent grain is observed.

Subplantation, in amorphous carbon films

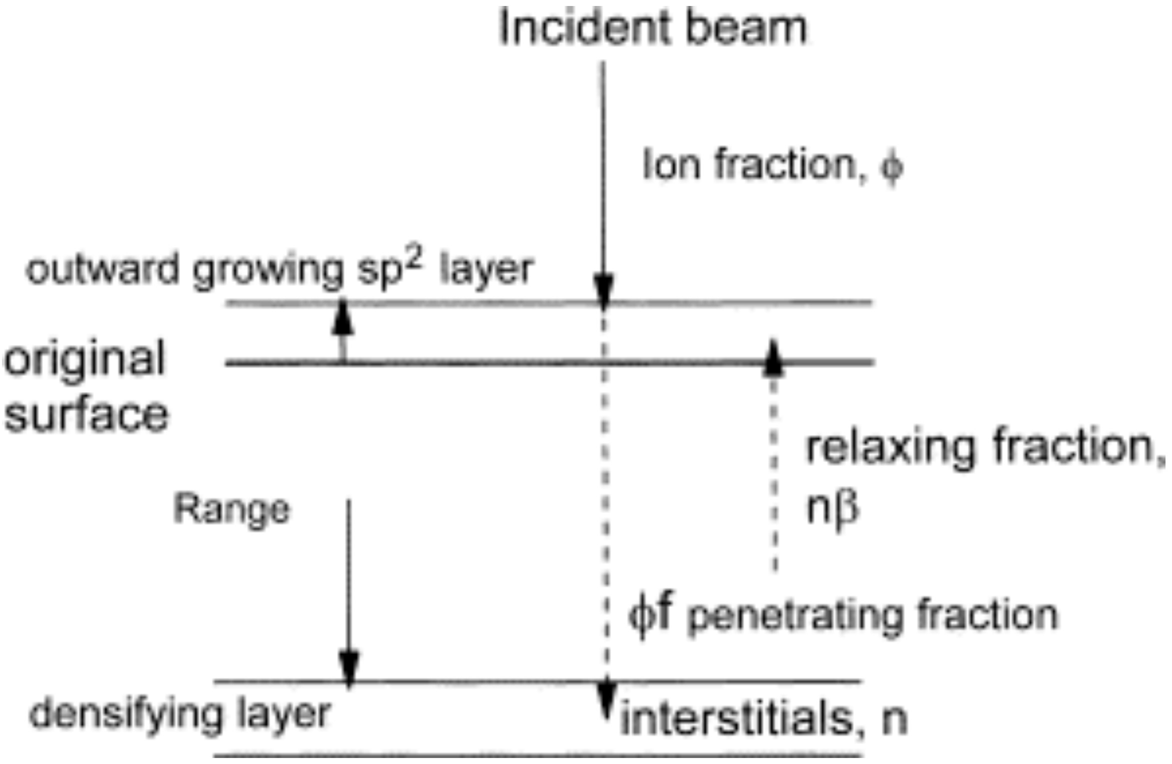

Schematic diagram of densification by subplantation. A fraction of the incident ions penetrate the film and densify it, the remainder end up on the surface to give thickness growth.

J. Robertson/Materials Science and Engineering R 37 (2002) 129–281

Subplantation -> Ion peening

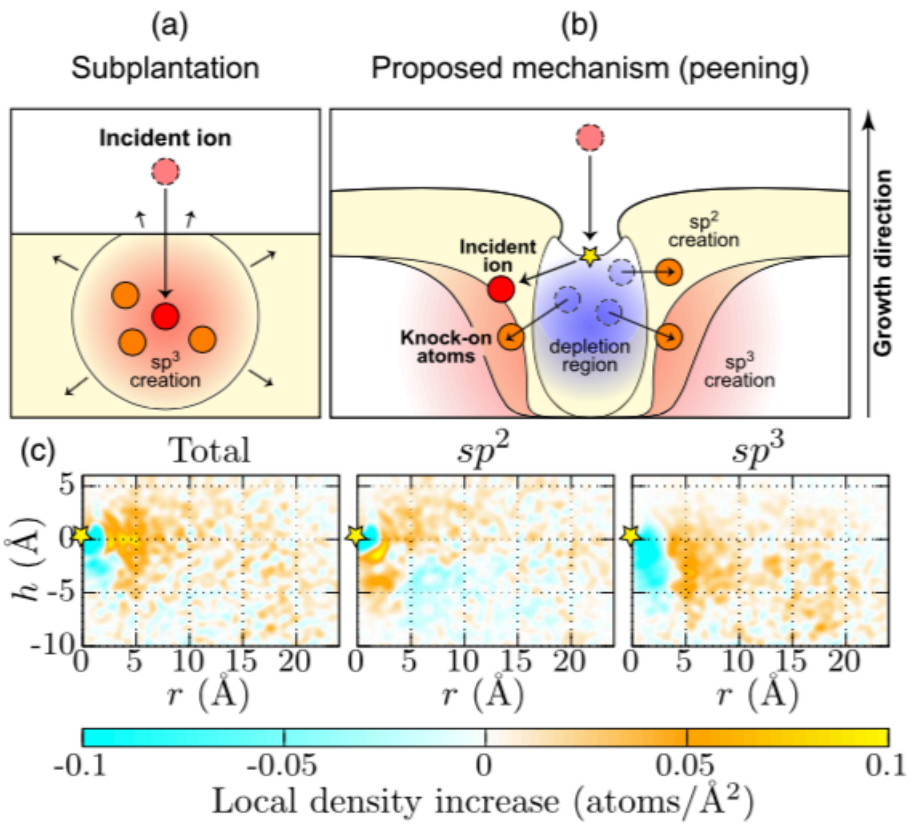

FIG. 4. (a) Previously accepted growth mechanism in ta-C and (b) growth mechanism proposed in this Letter. (c) Average increase in local mass density after ion impact (60 eV deposition; see text for details). The star indicates the impact site.

Miguel A. Caro, Volker L. Deringer,
Jari Koskinen, Tomi Laurila, Gábor Csányi,
PHYSICAL REVIEW LETTERS 120, 166101 (2)

Subplantation and experiments -Carbon

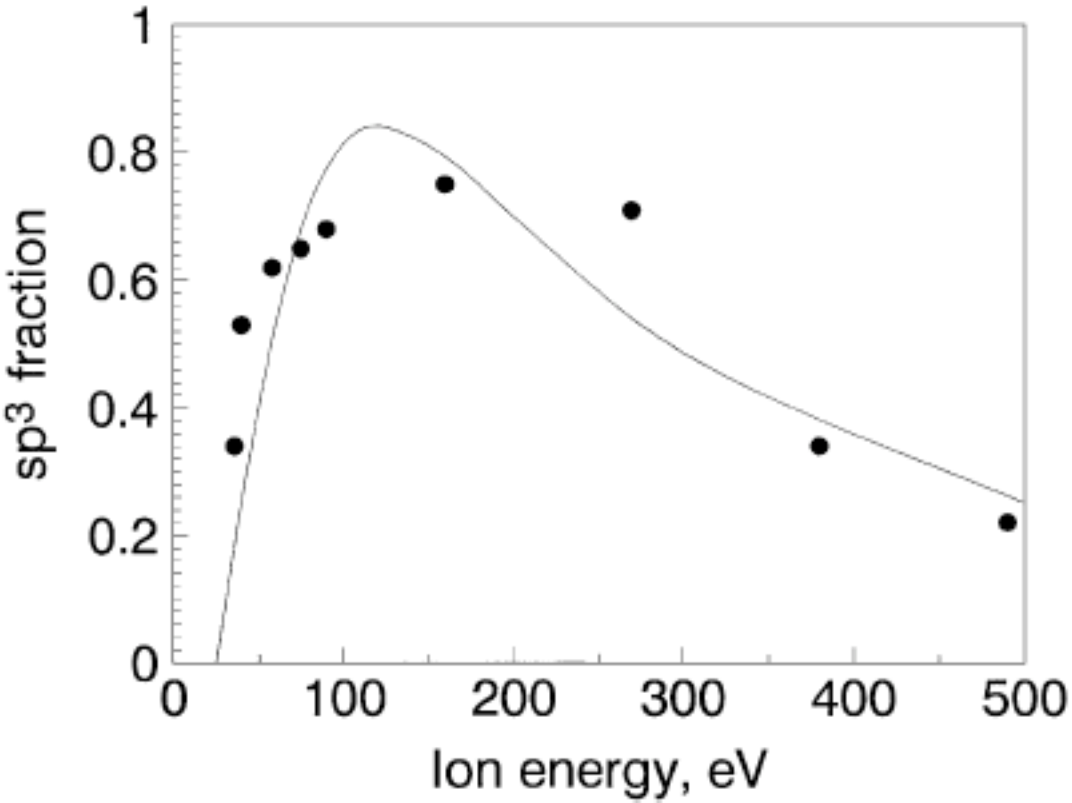

Comparison of calculated sp^3 fraction of ta-C according to subplantation model (Eq. (16)), with experimental data of Fallon et al. [17].

J. Robertson / Materials Science and Engineering R 37 (2002) 129–281

Ta-C film growth molecular dynamic simulation, Miguel Caro https://zenodo.org/record/1133425

In coming 100 eV carbon Ions

Growing film

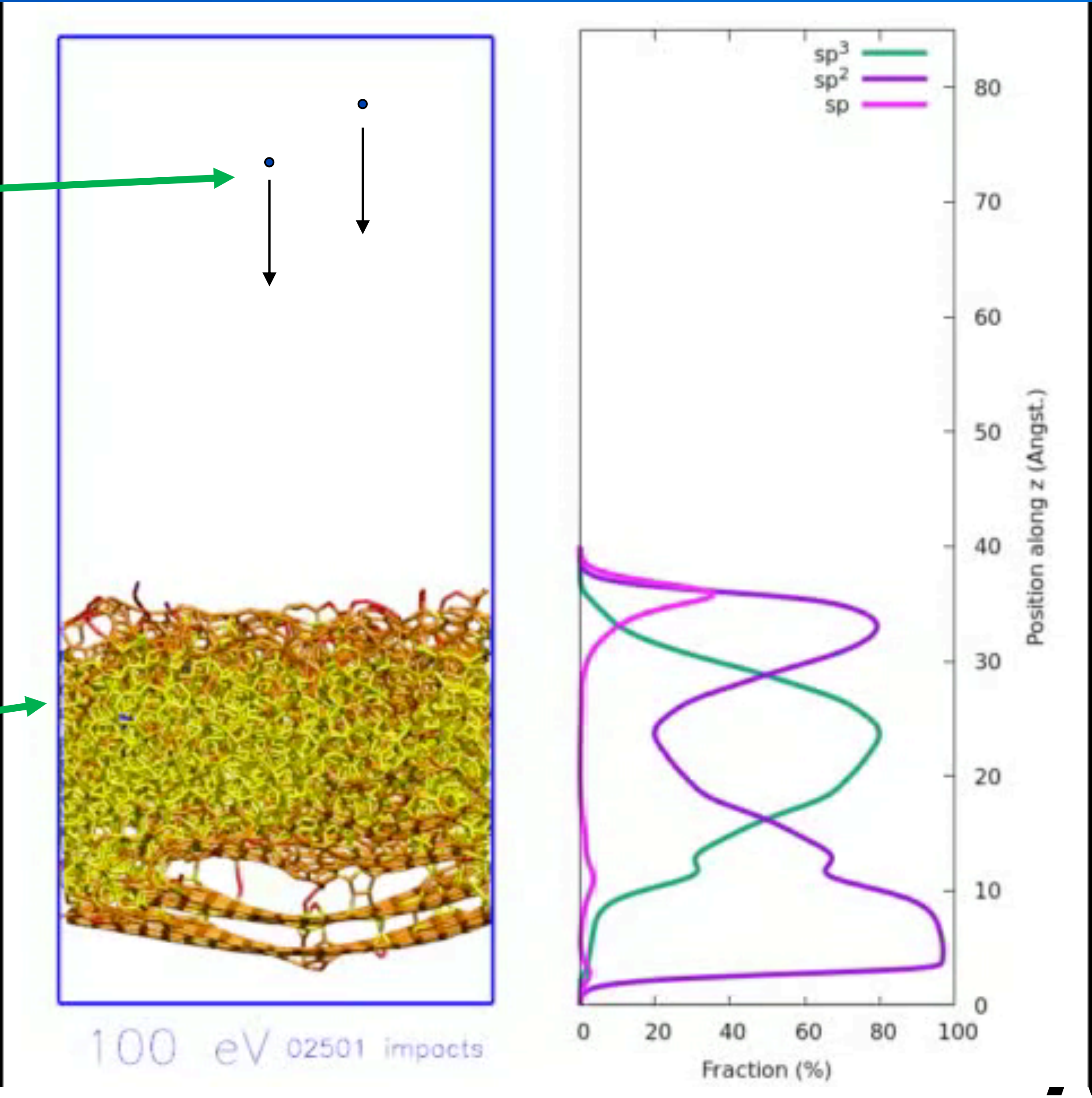

Ion bombardment

Effects to thin film properties:

Stress Control

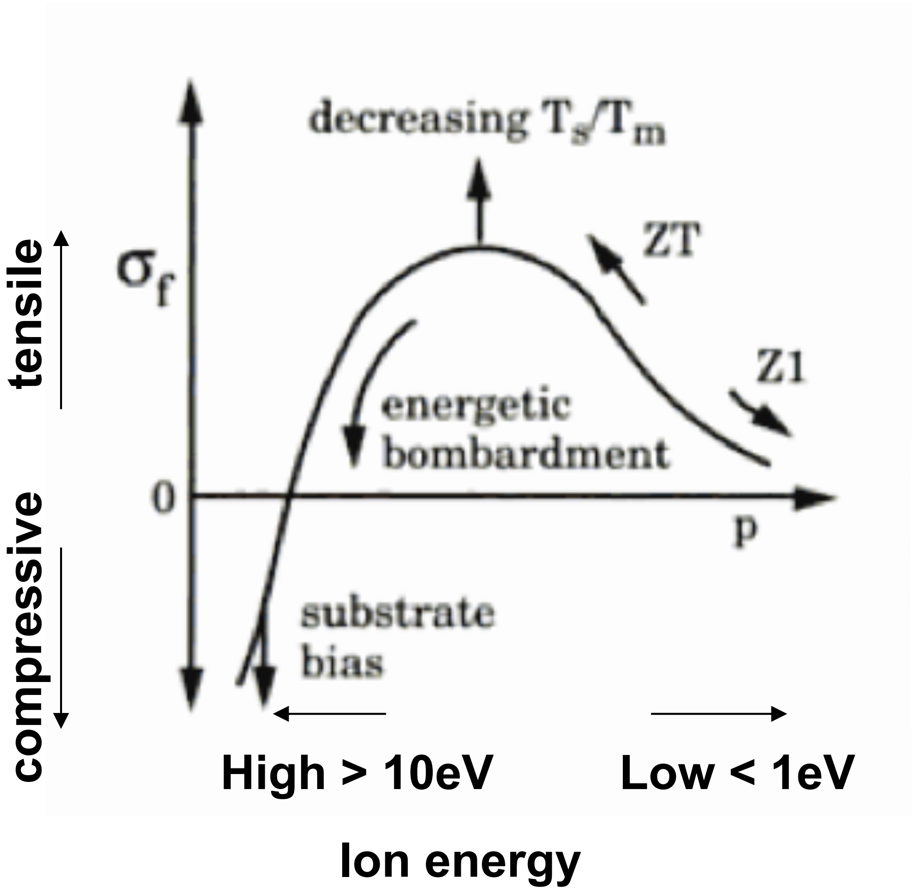

- Gas pressure /temperature
- Tensile stress due to collapsing of voids
- Higher temperature annealing of structure – low stress
- Compressive stress – subplantation

Surface roughness

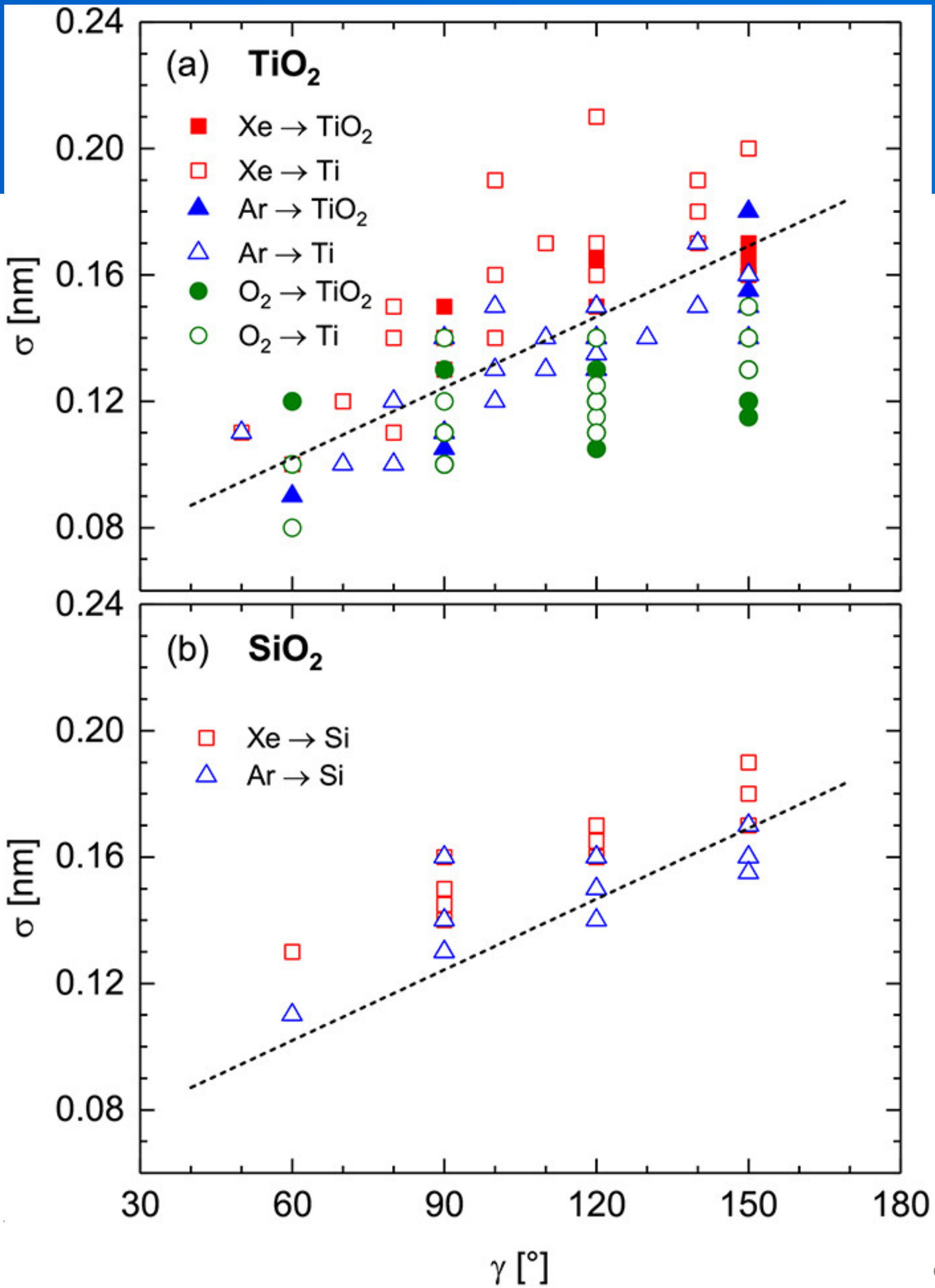

FIG. 22. Surface roughness σ versus scattering angle γ of TiO 2 thin films [panel (a)] and SiO 2 thin films [panel (b)] grown by reactive IBSD using process gas Xe (red symbols), Ar (blue symbols), or O 2 (green symbols) and a metallic target (open symbols) or a ceramic target (closed symbols). The dashed lines serve as a guide to the eye. Reproduced with permission from Bundesmann et al., Eur. Phys. J. B 90, 187 (2017). Copyright 2017 Springer (TiO 2 films, Ar and Xe ions, and TiO 2 target); Bundesmann et al., Appl. Surf. Sci. 421, 331 (2017). Copyright 2017 Elsevier (TiO 2 films, Ar and Xe ions, and Ti target); Pietzonka et al., Eur. Phys. J. B 91, 252 (2018). Copyright 2018 Springer (TiO 2 films, O 2 ions, and Ti and TiO 2 target); Mateev et al., Eur. Phys. J. B 91, 45 (2018). Copyright 2018 Springer (SiO 2 films).

Published in: Carsten Bundesmann; Horst Neumann; *Journal of Applied Physics* 124, 231102 (2018)
DOI: 10.1063/1.5054046
Copyright © 2018 Author(s)

Ion beam nano roughening

- **Enhanced adhesion**

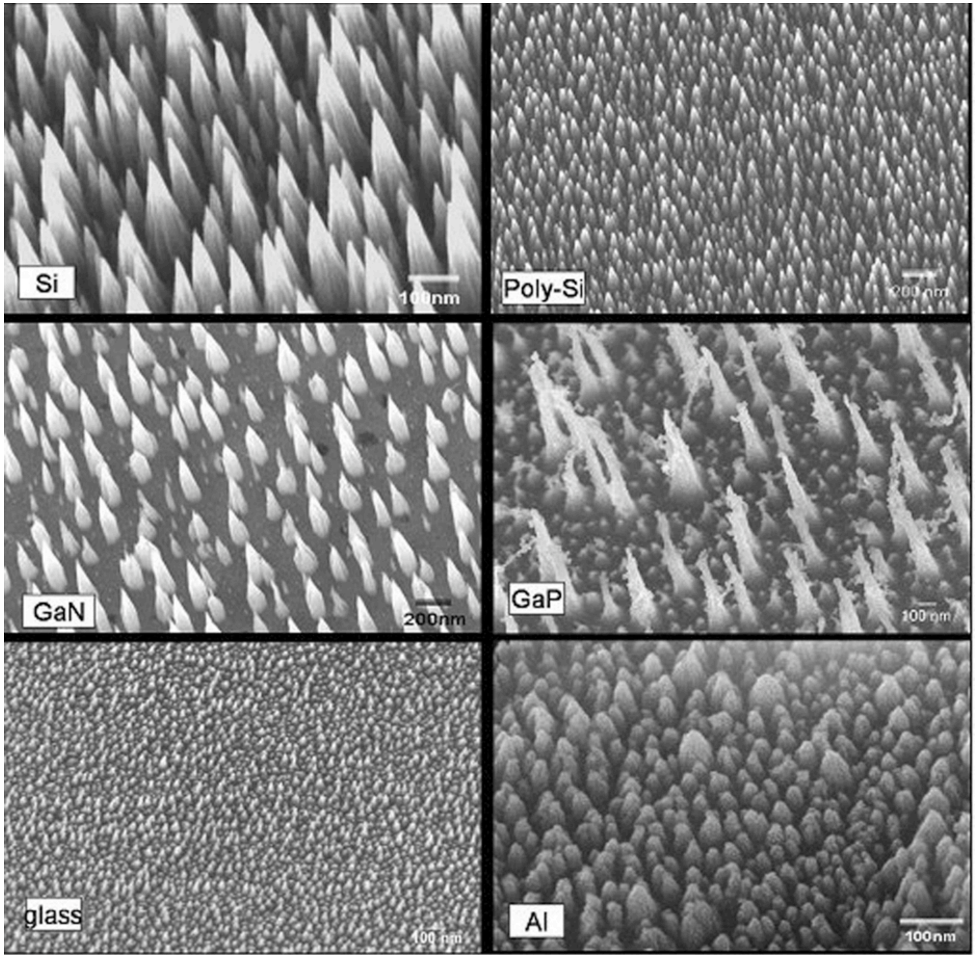

Index of refraction

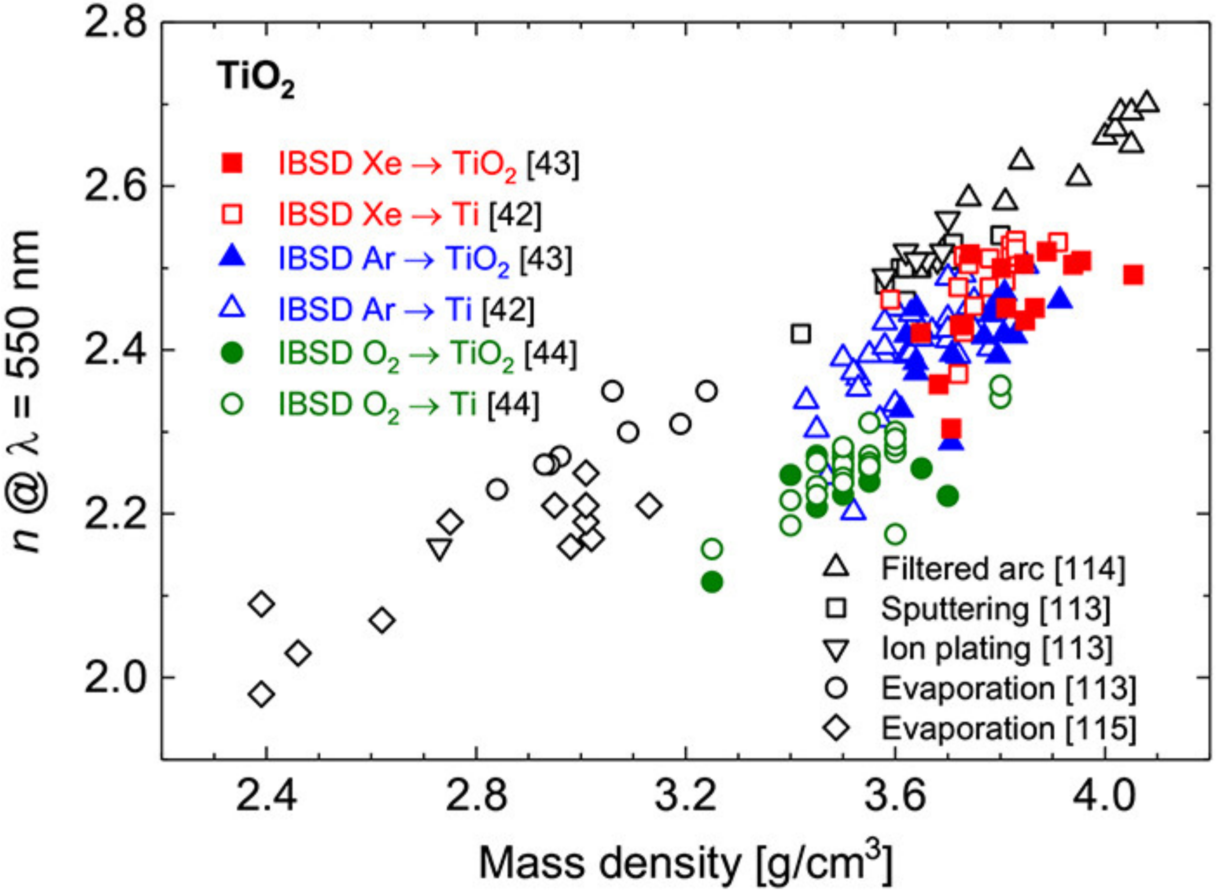

FIG. 24. Index of refraction n at λ = 550 nm versus mass density of TiO_2 thin films grown by various PVD techniques.[42–44,113–115] Reproduced with permission from Bundesmann et al., Appl. Surf. Sci. 421, 331 (2017). Copyright 2017 Elsevier.

Published in: Carsten Bundesmann; Horst Neumann; *Journal of Applied Physics* 124, 231102 (2018)
DOI: 10.1063/1.5054046

Electrical resistivity

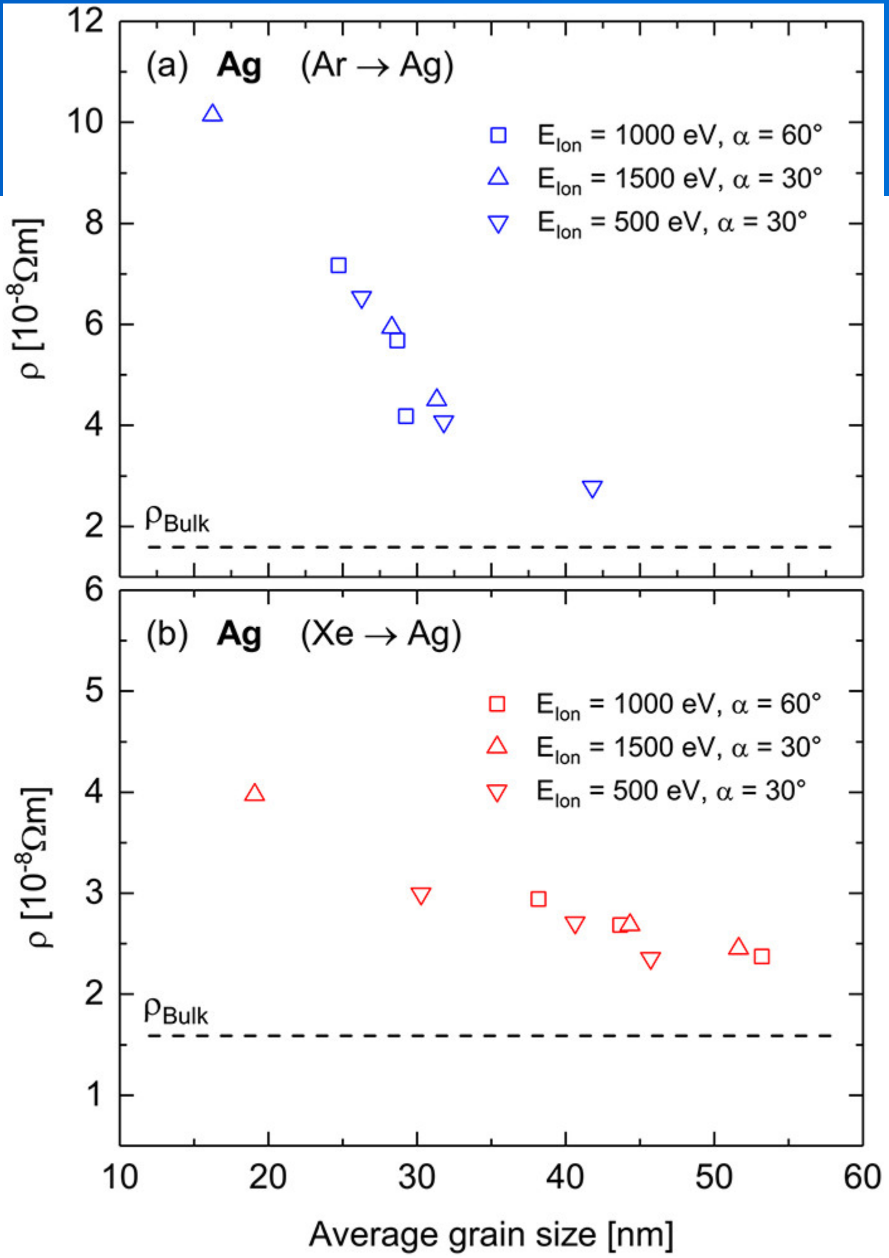

FIG. 20. Electrical resistivity ρ versus average grain size of Ag thin films grown by IBSD using Ar ions [panel (a)] or Xe ions [panel (b)]. Please note the different scales. The data are shown for different sets of process parameters (E Ion, α). The horizontal dashed lines indicate the electrical resistivity of Ag bulk. Reproduced with permission from Bundesmann et al., Thin Solid Films 551, 46 (2014). Copyright 2014 Elsevier.

Published in: Carsten Bundesmann;
Horst Neumann; *Journal of Applied Physics* 124, 231102 (2018)
DOI: 10.1063/1.5054046